

# A FEASIBILITY STUDY OF LASER-ASSISTED TITANIUM IMPLANT DRILLING FOR PERIPROSTHETIC FRACTURE REPAIR

A Thesis

by

CARLETON THOMAS VANGSNESS III

Submitted to the Office of Graduate and Professional Studies of  
Texas A&M University  
in partial fulfillment of the requirements for the degree of

MASTER OF SCIENCE

Chair of Committee,  
Co-Chair of Committee,  
Committee Member,  
Head of Department,

Bruce L. Tai  
Mathew Kuttolamadom  
Timothy Jacobs  
Andreas A. Polycarpou

August 2017

Major Subject: Mechanical Engineering

Copyright 2017 Carleton Thomas Vangsness III

## ABSTRACT

This body of work studies the feasibility of hand drilling through a titanium implant located in the femur. This is hypothesized to be achievable via laser-assisted drilling with carbide tools. A series of tests were conducted to measure the thrust force and torque with different shaped drill bits under dry- and laser-assisted drilling (using a 200-watt fiber laser), respectively. These drill bits included 2-flute and 3-flute twist drills and a straight flute drill that is clinically available. Successive time under laser exposure was examined. Thermal propagation was examined both experimentally and modeled in Abaqus. Finally, tool wear was examined. When all results are taken in context, the best option for clinical use is the two-flute design. The three-flute design is not practical for use during hand drilling and the straight flute experiences significant tool wear. Further, thermal control will need to be looked at due to a higher heat input from drilling than laser exposure.

## ACKNOWLEDGEMENTS

I would like to offer my thanks to all those who made my Masters of Science at Texas A&M University possible.

## CONTRIBUTORS AND FUNDING SOURCES

### **Contributors**

This work was supervised by a thesis committee consisting of Professor Tai, my advisor; Professor Kuttolamadom as my co-advisor; and Professor Jacobs of the Department of Mechanical Engineering.

Guidance on the clinical aspects of this project was provided by Dr. James Kellam.

All work conducted for the thesis was completed by the student independently.

### **Funding Sources**

This thesis was made possible by the donation of tooling from Kennametal and the use of lab facilities provided by Professor Wayne Hung.

# TABLE OF CONTENTS

ABSTRACT .....	ii
ACKNOWLEDGEMENTS .....	iii
CONTRIBUTORS AND FUNDING SOURCES .....	iv
TABLE OF CONTENTS.....	v
LIST OF FIGURES .....	vii
1. INTRODUCTION .....	1
1.1. Periprosthetic Fractures .....	1
1.2. Current Repair Methods .....	1
1.3. State of Current Patients .....	3
1.4. Objective .....	4
2. BACKGROUND RESEARCH .....	5
2.1 Current Obstacles .....	5
2.2 Previous Works .....	5
2.3 Proposed Solution .....	7
3. DRILLING FORCES: THRUST AND TORQUE .....	10
3.1 Experimental Design .....	10
3.2 Bit Selection .....	12
3.3 Human Test.....	14
3.4 Experimental Process .....	15
3.5 Data Analysis .....	16
3.6 Results .....	17
4. TOOL WEAR .....	23
4.1 Tool Wear.....	23
4.2 Tool Wear Causes .....	23
4.3 Tool Wear Analysis .....	24
4.4 Results .....	24
4.5 Discussion.....	26
5. THERMAL STUDY .....	27
5.1 Thermal Generation and Propagation .....	27
5.2 Abaqus Model .....	29
5.3 Inverse Plotting .....	32
6. DISCUSSION .....	36
6.1 Discussion.....	36

7. CONCLUSIONS AND FUTURE WORKS.....	38
7.1 Conclusions.....	38
REFERENCES .....	40

## LIST OF FIGURES

Figure 1. Coaxial drill with laser .....	8
Figure 2. Test Rig for Experiment .....	12
Figure 3. Three Kennametal solid carbide drill bits .....	14
Figure 4. Example of force data (after a 10hz low pass filter) .....	17
Figure 5. Axial force chart for cold & 80 sec laser exposure of all three drill bits .....	18
Figure 6. Torque chart for cold & 80 sec laser exposure of all three drill bits .....	19
Figure 7. Axial force chart for cold, 20 sec, & 40 sec laser exposure of all three drill bits .....	20
Figure 8. Torque force chart for cold, 20 sec, & 40 sec laser exposure of all three drill bits .....	20
Figure 9. Tool wear present on straight flute bit .....	24
Figure 10. Tool wear present on two-flute twist bit .....	25
Figure 11. Temperature calibration results of two tests. TC 1 is placed at 1 mm from the laser spot for the first test, 3 mm for the second test. TC2 is replaced at the same distal edge for both tests. ....	28
Figure 12. Top down view of thermocouple locations .....	28
Figure 13. Model of titanium workpiece .....	29
Figure 14. Axisymmetric model & meshed model .....	30
Figure 15. Location of heat flux on the model representing the laser .....	31
Figure 16. Location oh heat flux representative of drilling .....	31
Figure 17. Overlay of experimental temperature data with theoretical data outputted from the model for the laser .....	33

Figure 18. Overlay of experimental data and theoretical model output for drilling .....	34
Figure 19. Thermal propagation while drilling .....	35



# 1. INTRODUCTION

## 1.1. Periprosthetic Fractures

Bone fractures located near implants, known as periprosthetic fractures, are some of the most difficult fractures to repair. They are most commonly located in the femur near the stem of a hip implant or in the tibia at the location of a knee implant. Periprosthetic fractures are classified using the Vancouver ranking system, broken down into three categories, “Type A occurring around the trochanteric region, Type B near or just distal to the femoral stem, and Type C well below the femoral stem.” These fractures are further subdivided based on stability and bone stock; “Type B fractures: B1 implies a well-fixed stem, B2 a loose stem with good bone stock, and B3 designates poor surrounding bone stock”. Both Type B and Type C fractures are treated with surgical repair; Type A fractures can often be treated without surgery by using medical management and keeping the affected limb from bearing weight.

## 1.2. Current Repair Methods

There are several different types of repair methods that can be used to fix long bone fractures. Depending on the location of the fracture and implant, an intramedullary pin or nail can be used. These are solid stainless steel or titanium pins that are driven into the medullary cavity of a bone. They can be used in conjunction with other types of repair methods for added fracture support and stability.

If a pin is not suitable for the location, locking plates can be used. These are stainless steel or titanium plates that are placed such that they span the fracture, holding the once displaced pieces of bone in apposition. Locking plates are secured in place using a variety of anchors [1-5]. The most common method of anchoring locking plates is using screws. There are several different types of surgical screws, but the two most commonly used are cortical and cancellous screws. Cortical screws span the medullary cavity of the bone and engage cortical bone on both sides. They have closed space, shallow threads with blunt ends. Cancellous screws are constructed for fixation of cancellous bone, a spongy mature bone often found in the end of long bones, such as the femur. They have much wider thread spacing than cortical screws and are weaker when compared to cortical screws with the same outside diameter. Nearly all screw designs in use today are self-tapping, which is the recommended technique for applying bone screws during surgery.

Cerclage wire is typically used to correct long oblique fractures or when the angle at which a fractured fragment must be held cannot be achieved with a plate or intramedullary pin. This is the least ideal form of anchoring because they must be placed slowly and can potentially cut off blood flow to the healing bone which can lead to tissue necrosis.

The vast majority of periprosthetic fractures require surgical repair. This is due to the extreme structural damage to the bone and the presence of an existing bone implant limiting the types of fixation that can be used to correct the fracture.

If the fracture is not near an implant, the repair is straightforward: a metal rod can be inserted into the femur to stabilize the fracture, and if necessary, additional plates can be attached to the bone with screws to provide more fracture stability. If the fracture is too close to the implant, this method of fracture repair is not possible; the implant occupies the space where the rod or screws would be inserted into the bone. Sometimes, screws can be set into the cortical bone near an implant at an angle, though this severely diminishes the strength of the anchor.

In cases in which screws cannot be used, the alternative method for securing a locking plate is with cerclage wire. A prime example of one of these cases is in elderly patients, the most common group having periprosthetic fractures. Many of these patients also have osteoporosis; this carries an increased risk of mechanical failure of a plate with screws due to the structural weakness of the surrounding bone [6]. Despite the risks associated with using cerclage wire, it is often a necessity in these cases where using a screw is likely to do more harm than good.

### 1.3. State of Current Patients

As the technology used in the design and placement of implants has advanced, the number of people receiving total hip and total knee replacements has increased. This is seen in middle aged people who have an active lifestyle. [10] People in this age group are the most likely to receive a total hip or total knee

replacement, but if they continue their active lifestyle after joint replacement surgery, this predisposes them to periprosthetic fractures.

The other group of people predisposed to periprosthetic fractures are the members of the aging baby boomer generation. Medical advances have led to longer lifespans and more active lifestyles for older people. Because of this, there has been an increase in the number of elderly patients with worn out joints. The US census bureau estimates that the population of people over the age of 65 will reach 90 million or more by the year 2050. [1] Due to the prevalence of osteoporosis in this age group, the current anchoring techniques used during surgical repair do not offer the desired when fixing a fracture. [7-9].

#### 1.4. Objective

Currently, most periprosthetic fracture repairs are accomplished by setting screws angled into the cortical bone around the implant, locking the plates into place. An ideal solution would be drilling and anchoring screws directly into the implant, thereby addressing the issues of weak bone structure (found in elderly and osteoporotic patients) and reducing complications from current anchoring techniques. However, this is not possible with a regular surgical hand drill and stainless-steel drill bit; the implant material is usually made of titanium or cobalt chromium alloys which are typically difficult to machine. To make this solution feasible, this study aims to explore a laser-assisted drilling process along with different drill geometry designs adapted from the manufacturing industry.

## 2. BACKGROUND RESEARCH

### 2.1 Current Obstacles

Currently, a significant problem with this proposed solution, from a clinical perspective, is that the vast majority of tooling used in operating rooms is stainless steel. Not only is titanium an extremely tough material, it also work-hardens very quickly; stainless steel tool bits cannot drill into titanium with any reasonable amount of success. An additional complication is that most drills used during operations are extremely high RPM drills that have a very low torque output; these non-industrial drills are incapable of producing the force necessary to drill through tough materials like titanium.

### 2.2 Previous Works

Lasers are increasingly deployed in the supporting roles of machining difficult materials. They are used to heat the material, such as Inconel or titanium alloys, immediately preceding the cutting edge of the tooling. The localized energy input reduces the strength of the material, allowing for a force reduction of at least ten percent on the cutting edge while significantly extending the life of the tooling, and thus decreasing manufacturing costs. The high-powered laser typically heats the material in excess of 1000 °C during turning applications on a lathe, though research has also been done to examine the possibility of laser-aided machining using a lower powered laser for milling [11].

Dry machining of titanium alloys is well-documented, as it is a ubiquitous industrial application [12-19]. This includes not only turning and milling, but dry drilling of titanium [20]. Current research on laser-assisted machining is oriented towards improving the overall machinability of difficult-to-machine materials and thereby increasing productivity. For example, Chang and Kuo observed higher material removal rates when a ceramic was treated via laser while machining [21]. In addition, there has been research demonstrating a reduction in cutting force when treated by a laser [22, 23]. When the system was optimized for the distance of the laser projection and feed rate, a significant force reduction was observed by Ayed et al. [24]. Shun confirmed this in a reduction of feed force when milling Ti-6Al-4V after laser treatment [25]. Furthermore, the heat propagation of laser machining has also been extensively studied: Suthar et al. [26] considered laser intensity cutting speed, depth of cut, etc. on the effectiveness of laser-assisted machining (LAM). Both Yang etc. [27] and Joshi et al. [28] conducted numerical analysis on the effects of 3D heat propagation through titanium [28]. Finally, the effects of more power resulting from different strengths of lasers have also been studied (Rashid et al. [29]), with Rashid et al. recommending a range of 800 to 1200 W following an observational study on varying powers of lasers in the assistance of machining titanium [30]. This research demonstrates that the machining of titanium with lasers in an industrial setting has been well-documented with most laser powers having been in the 1 kW or greater range, purposed for heavy-duty machinery. However, little, or probably none, research

has been conducted using low-powered lasers (*e.g.*, several hundred watts) as methods of arresting heat propagation during surgery on live bodies.

The end goal of this project is to drill in living tissue, therefore thermal energy propagation and management during the drilling process must be taken into consideration. The FDA has a limit on both the temperature levels that can be reached during a procedure and amount of time tissue can be exposed to specific temperatures. Due to the extensive commercial use of titanium, its thermal properties have been studied intensively and are well understood. Several researchers have looked at the propagation of thermal energy through titanium in 3D space. These previous studies give us an understanding of how heat propagates through titanium in three dimensions and thus the ability to closely approximate the temperature at a site where it would be impossible or impractical to collect temperature data when drilling into titanium.

### 2.3 Proposed Solution

This study's proposed solution for the repair of periprosthetic fractures is the direct drilling and tapping of an intramedullary bone implant in order to anchor an interlocking plate directly into the existing intramedullary pin. This would reduce the need for multiple anchor types (such as a combination of cortical screws and cerclage wire) and would mitigate the issues posed by osteoporosis in elderly patients. To do this, we first needed to determine the conditions under which this would be possible.

This body of work presents a preliminary effort to understand potential force reduction in laser-assisted (maximum 200 W) titanium drilling as well as associated temperature propagation. This is the first step towards an integrated laser-drilling system and parameter optimization. The final step would be the design and construction of a coaxial laser and drill, such as shown in Figure 1. This device would contain a hollow drill bit in which a laser is projected through, allowing for simultaneous heating of the titanium implant while cutting away this softened material.

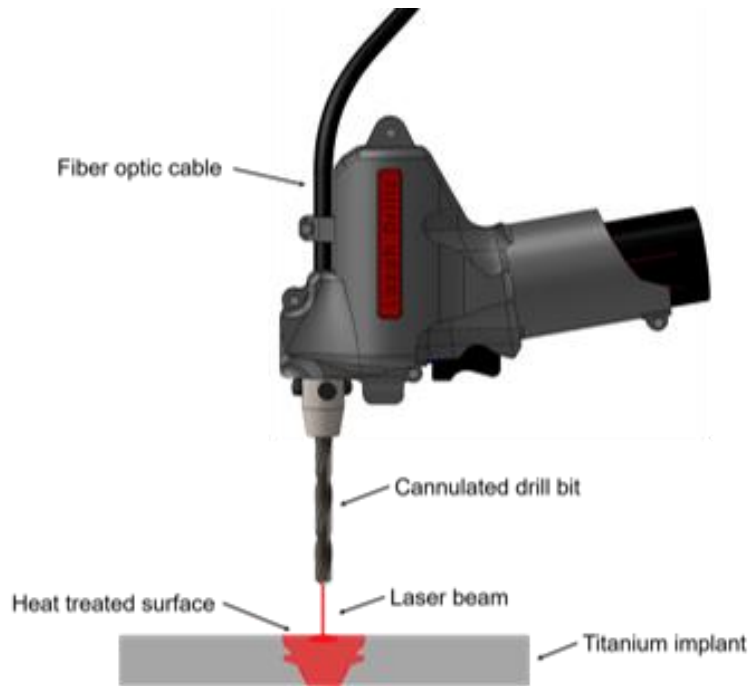


*Figure 1. Coaxial drill with laser*

The following sections of this paper, will specify the experiments and data analysis, compare different drill bits and laser treatments, look at tool wear, and



discuss thermal propagation and generation both experimentally and in theoretical modeling. In addition, clinical aspects and application of results are considered.

### 3. DRILLING FORCES: THRUST AND TORQUE

#### 3.1 Experimental Design

There were multiple independent and dependent variables analyzed when studying the forces present during drilling. The first factors investigated were the forces present in the axial direction when drilling in the test rig and the torque values experienced by the operator of the drill. The RPM of the drill bit and the feed rate of the bit into the workpiece were two controlled variables throughout the study. It was also important to determine if there was enough space to have the laser tip close enough to the workpiece to be within the focal distance of the laser but still far enough that the heated area could then be drilled.

To perform initial verifications, the testing apparatus was constructed as shown in Figure 1. A common hand drill (Chicago Electric Power Tools 61714) capable of accepting various bits was selected. This drill differs from those currently available to surgeons because it has an additional speed reduction device that increases the available torque and reduces the risk of the drill stalling during the operation. The drill is attached to a linear slider (Moog Animatics L70) to ensure that it is perpendicular to the workpiece and to remove the instability associated with drilling by hand. The titanium sample is a cylindrical shape of 25.4 mm diameter with two flat faces for clamping with the vise (Figure 1). The top surface is faced to be perfectly flat and then peck drilled to avoid the drill wandering at the point of contact along with having full flute engagement upon contact. The sample is then clamped in axial alignment with the drill bit.

Specifically, the titanium used is Ti-6Al-4V alloy, which is the primary composition in a hip prosthesis (the body) in conjunction with cobalt chromium alloy (the head). Torque and force readings are taken via a Kistler piezoelectric dynamometer (Model 9272). A 200-watt continuous fiber laser (IPG 200-watt YLR-SM Ytterbium fiber laser) is mounted in a HAAS VF-1 CNC machine, allowing control of the laser's power and for holding an accurate distance from the workpiece as the laser tip is moved. In experiments, the laser is applied on the workpiece for a period of time and then moved away from the center location as soon as the drill is fed into the workpiece. To monitor the temperature of the heated spot and the entire workpiece, a K-type thermocouple (Omega Engineering 5TC-TT-K-36-36) is placed on the distal edge of the workpiece. It is used to estimate to the center temperature during the heating process, based on a separate calibration test between two thermocouples with one close to the workpiece center and one on the distal edge (shown in Results section).

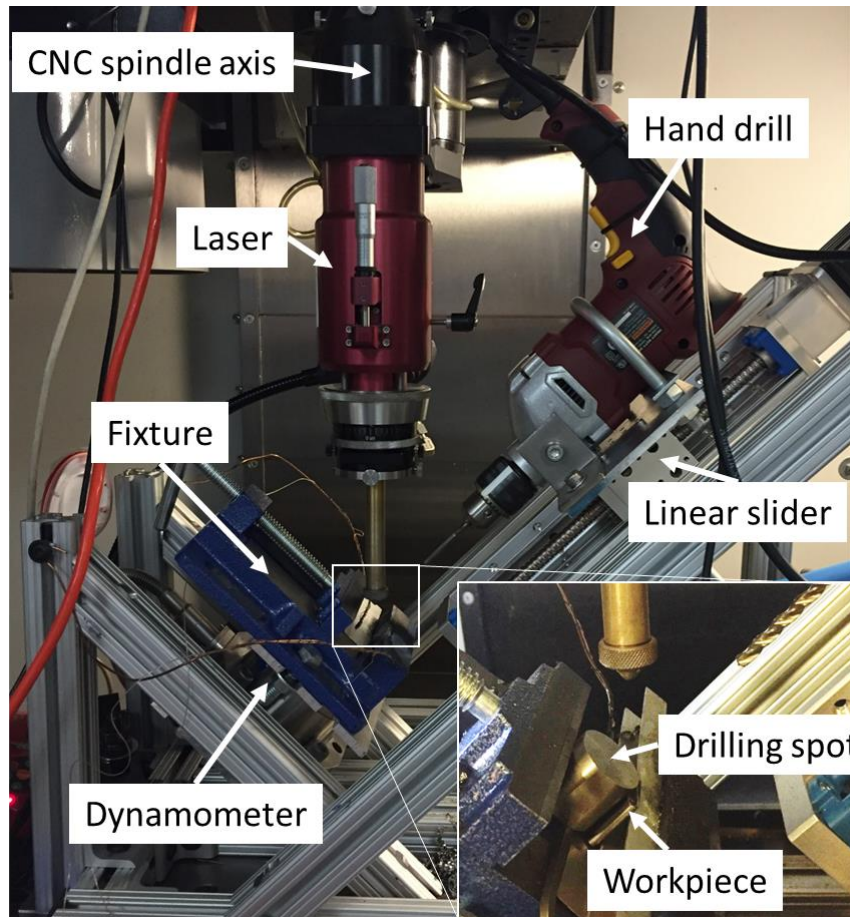


Figure 2. Test Rig for Experiment

### 3.2 Bit Selection

When deciding which bits to use in this experiment, several factors were considered. First and foremost, it was imperative to determine which materials are approved for surgical use by the FDA in the human body. Almost all forms of commercially available carbide are FDA approved for use in humans. Next, the types of drill bits currently being used in the operating room were assessed. Straight flute, zero rake drill bits are the main types of bits used, and these come

in a variety of materials that can be autoclaved. Lastly, cutting edge technology found in industrial machining was considered. Two and three flute drill bits are the most commonly used drill bits in industrial machining.

Three different solid carbide drill bits of 5 mm diameter, provided by Kennametal (Latrobe, PA) are analyzed here. The first is a straight flute zero rake drill bit (Model B411A05000 KF1) with a material upgrade to carbide to better handle the rigors of cutting a material as hard as titanium. It is often used for pilot hole drilling on a stock material that requires the strength to prevent bending. This type of drill is also available in clinical use, for example Synthes' (West Chester, PA) Carbide Drills for screw removal. The second was a standard two flute twist drill bit (Model B052A05000CPG KC7325) with a 140-degree point that has a Titanium Aluminum Nitride (TiAlN) coating to add in reducing friction and increasing durability at elevated temperatures. The third drill bit is a three-flute twist drill bit in carbide (Model B105F5000 K10) designed for drilling tough materials. This drill bit can theoretically increase drilling efficiency by reducing the chip load from the cutting edge.



*Figure 3. Three Kennametal solid carbide drill bits*

### 3.3 Human Test

The first step taken was to quantify the force that the average human produces when drilling. To do this, the test rig was configured to approximate the position of a person drilling at waist level to replicate a real world surgical situation. A metal dowel was placed in the drill chuck to replicate a drill bit penetrating the workpiece. Pressure was then applied and held for ten seconds to determine a maximum level of force production. This test was repeated five times. After conducting all five experiments, the calculated average force value in the axial direction was 460 newtons.

### 3.4 Experimental Process

Process variables during drilling include drill type, size, feed rate, spindle speed, laser power, and exposure time. In this pilot study, drill feed rate and spindle speed were kept constant. The drill was fixed at full speed of 980 RPM. The feed rate of 0.0153 mm/rev was used to ensure the thrust force below 800 N, which was the linear slider's safety limit.

The laser power and exposure time were also controlled at 200 W for 80 seconds to reach a maximum temperature around 800°C at the focusing spot. The counterpart comparison was dry drilling without laser assistance. Each drilling was repeated three times, with and without the laser assistance. Only one laser exposure was used (200W for 80 s); therefore, there was a total of three by two tests.

Since the peak force produced by most drills is less than the maximum power output of a human, different laser exposure time intervals were used to further analyze the force reduction. Absent from these follow up experiments is the three-flute bit. Due to the high force levels generated by its use and its stalling of the linear slider (indicating a force level of over 800 N) it was determined that there is not enough power to successfully utilize the three-flute design outside of an industrial machine.

In performing these tests, a new drill bit was first drilled down five millimeters. Then the workpiece was changed out. The new workpiece was exposed to the laser for 20 seconds, then drilled five millimeters. The workpiece was changed out

a second time, exposed to the laser for 40 seconds, then drilled to a depth of five millimeters. This procedure was repeated three times for each bit. This specific procedure was established to mitigate the significant tool bit wear that was observed in previous experiments

### 3.5 Data Analysis

Figure 3 shows a typical thrust force obtained from a drilling test. The torque data has a profile similar to that seen in the figure, where the magnitude increases at the beginning and reaches a plateau as the drill bit fully engages. In some cases, the plateau is not clear, but the transition to the full engagement can still be seen. For analysis, the thrust force and torque are taken from the average of the selected length in the middle of fully engaged region where the drill bit is being fed at a steady rate. This region represents a steady-state drilling, and is a common way of evaluating drilling tools, as shown in Figure 3.



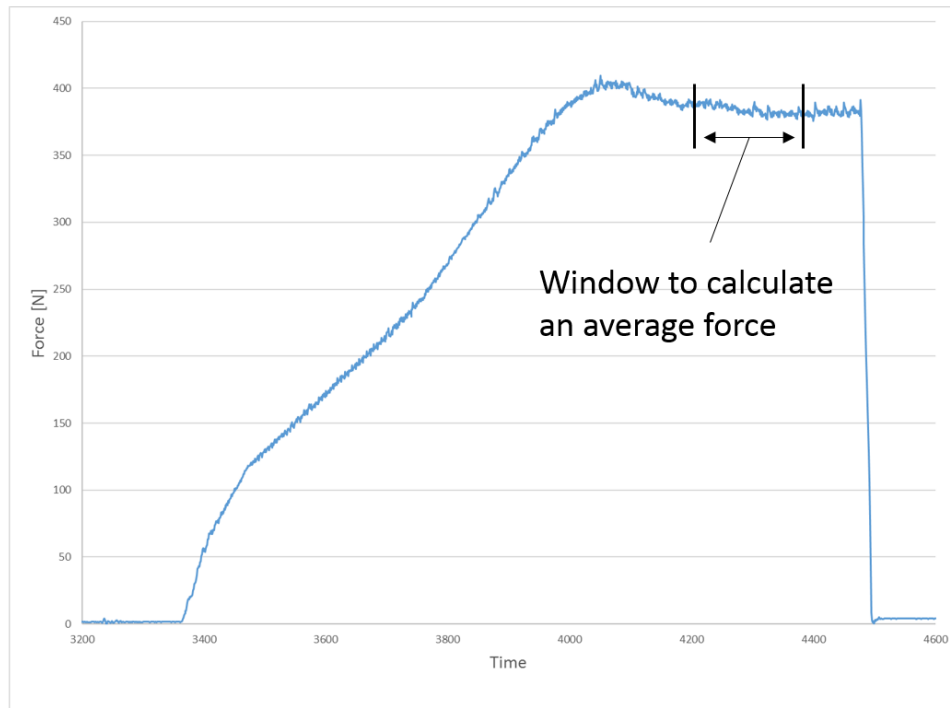


Figure 4. Example of force data (after a 10hz low pass filter)

### 3.6 Results

Thrust and torque forces present after the drill bit was fully engaged in the workpiece were analyzed in these results. Thrust force results for all experiments are shown in Figures 5 & 7. The error bar represents one standard deviation, which was calculated by using the data collected from all three trials for each drill bit. The two-flute drill bit outperformed the other two bits in both the non-laser and laser trials. For the two-flute bit, the laser reduces the force by approximately 10% when compared to the non-laser force. The three-flute drill has a much higher force (over 500 N) and fairly large variation. The peak force is high enough to potentially stall the linear slider, but a significant reduction in force (more than

30%) is observed when drilling is assisted by the laser. In comparison, the straight flute drilling does not seem to be affected by the laser – the thrust force remains around 370 N in both cases.

The overall trend of the torque data is similar to the trends seen in the force results; the two-flute bit is the best option, as shown in Figure 6. Torque was slightly reduced (less than 10%) for both two-flute and three-flute drills, but was drastically increased for the straight flute bit. This indicates that using the straight flute bit to drill in the laser-treated titanium is highly inconsistent. This is likely due to material build-up and/or chip accumulation at the cutting edges of the drill bit.

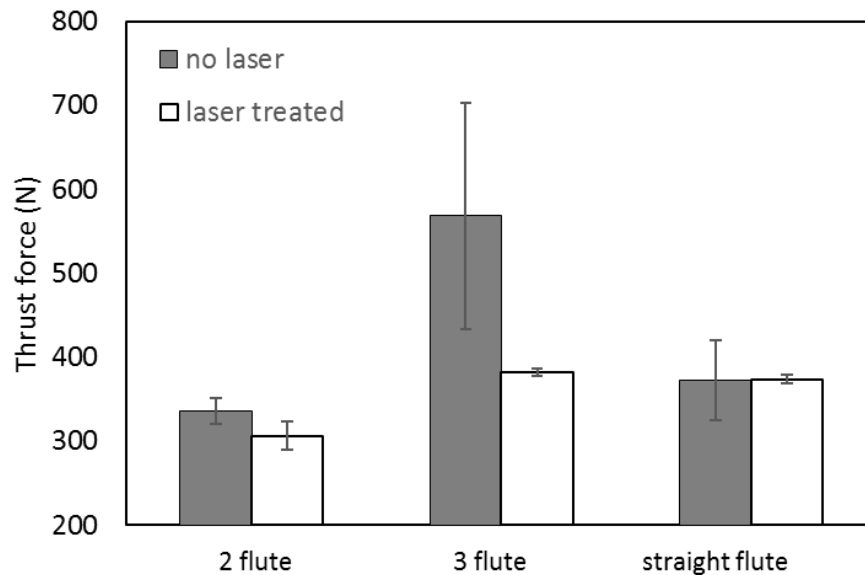


Figure 5. Axial force chart for cold & 80 sec laser exposure of all three drill bits

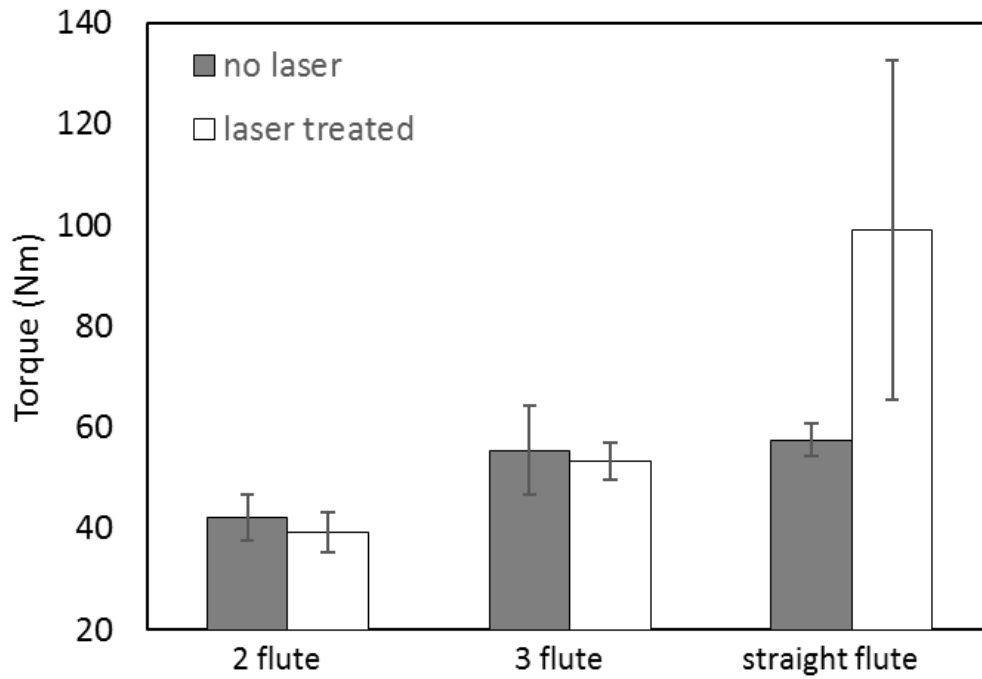


Figure 6. Torque chart for cold & 80 sec laser exposure of all three drill bits

After analyzing the first set of experimental results, a second set of experiments were conducted to assess the force reduction possible when using a smaller laser treating interval. The results are presented below.

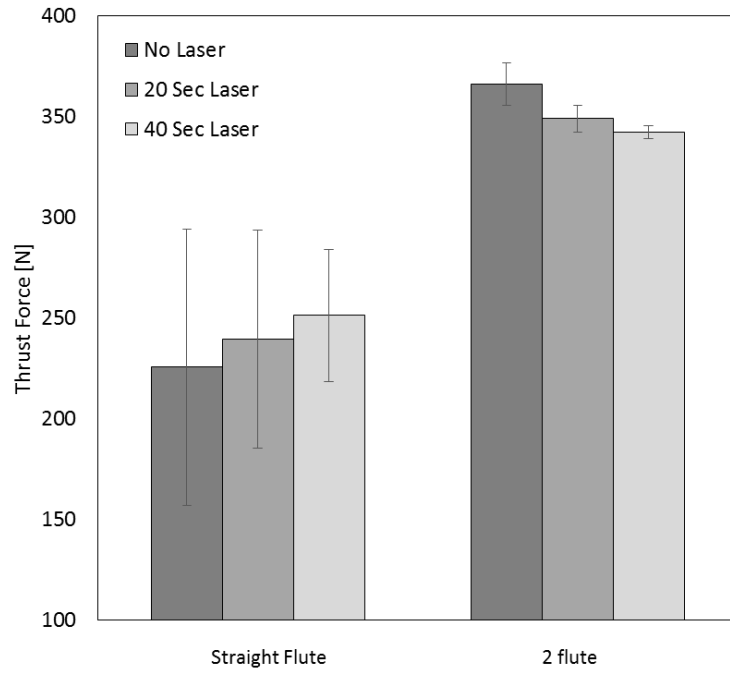


Figure 7. Axial force chart for cold, 20 sec, & 40 sec laser exposure of all three drill bits

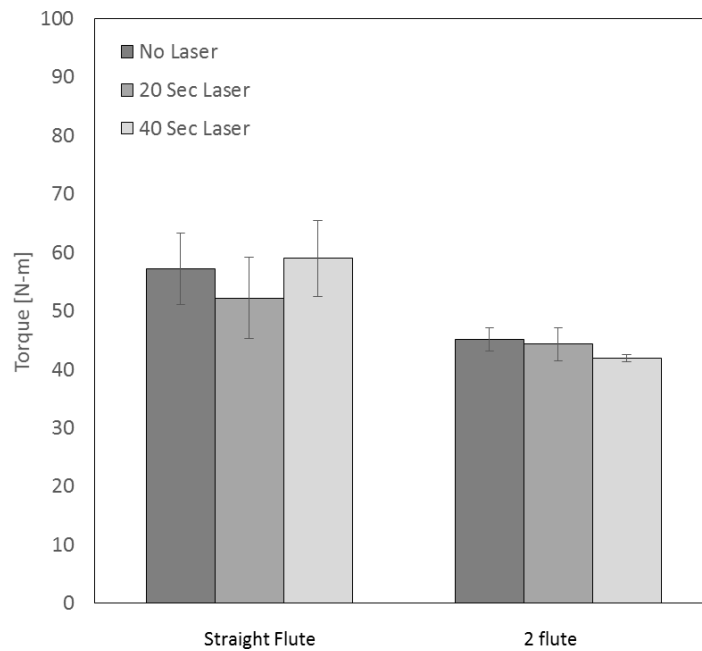


Figure 8. Torque force chart for cold, 20 sec, & 40 sec laser exposure of all three drill bits

The straight flute design, as a new bit, showed an extremely low amount of axial force needed to produce the required hole depth as shown in Figure 7. The force generation increased as the workpiece was exposed to the laser for longer, though this was negligible overall. This could be attributed to the 'gummy' nature of titanium at elevated temperatures coupled with the lack of chip evacuation due to the straight flute design or to degradation of the cutting edge. Further tests would need to be conducted with new bits to determine the effects of tool wear on the results.

The two-flute bit follows a similar trend of a slight decrease in force when exposed to the laser, though the force reduction was less than 10 percent overall. The deviation between tests is significantly lower than the straight flute bit, either due to less edge degradation or better chip evacuation making the force more consistent.

Overall, both cold and laser exposed drillings are below the level of human force production. The straight flute bit had a force requirement of approximately 64 percent of the two-flute bit, though with extremely high deviations. When looking at the torque values for the second round of testing (shown in Figure 8), we see values similar to the first round of testing when cold. The straight flute torque is roughly 140% higher than that of the two-flute. This is a very large perceived difference when controlling the drill itself. Furthermore, there is not a significant increase in torque as seen in the 80 second test due to the fact that the

titanium temperatures have not yet reached the point where it has melted or become 'gummy'. This means that chip evacuation with the straight flute bit is still happening or is not an issue at these relatively cold temperatures. The standard deviation is lower, also indicating that it is possible that the torque value is being generated by heavy wall friction in addition to the shear cutting mechanics. The two-flute bit followed a trend similar to that seen in the first experiment with a negligible lowering of torque due to laser exposure. This can mostly likely be attributed to efficient chip evacuation due to the twisted flute design

## 4. TOOL WEAR

### 4.1 Tool Wear

A consideration related to clinical use of these tool bit is how many holes per bit can be had due to their high cost.

### 4.2 Tool Wear Causes

There are several factors that contribute to tool wear. Flank wear is caused by regular erosion of abrading materials. This is the ideal wear pattern as it is controllable and predictable. Crater wear is localized on the rake face, commonly caused by a chemical reaction or excessive feed rate, leading to edge fracture. Build up is a form of pressure welding, very commonly found in stick materials such as stainless steel, aluminum, or titanium. Notch wear is excessive localized damage, often caused from the cutting edge contacting a work harden section of the workpiece. Thermal cracks are the result of the cutting edge going quickly from hot to cold and back again and often occur because of excessive vibration and chatter. Edge chipping is a complete degradation until failure of the cutting-edge due to the previous factors, eventually propagating until you are left with little to no cutting edge. Tool wear leads to an increase in cutting forces, increased temperatures of both the tool and workpiece due to friction, lower accuracy of finished dimensions, and ultimately tool breakage

### 4.3 Tool Wear Analysis

Due to the high cost of all bits used in this experiment, it was necessary to assess how wear from repeated use affected the forces produced by the bits when drilling. Using new bits, the bits were drilled five millimeters deep into the titanium stock, first at room temperature, followed by a twenty second laser exposure, then a forty second laser exposure. This set was repeated three times, for total of nine drills at a combined drilling depth of 45 millimeters.

### 4.4 Results

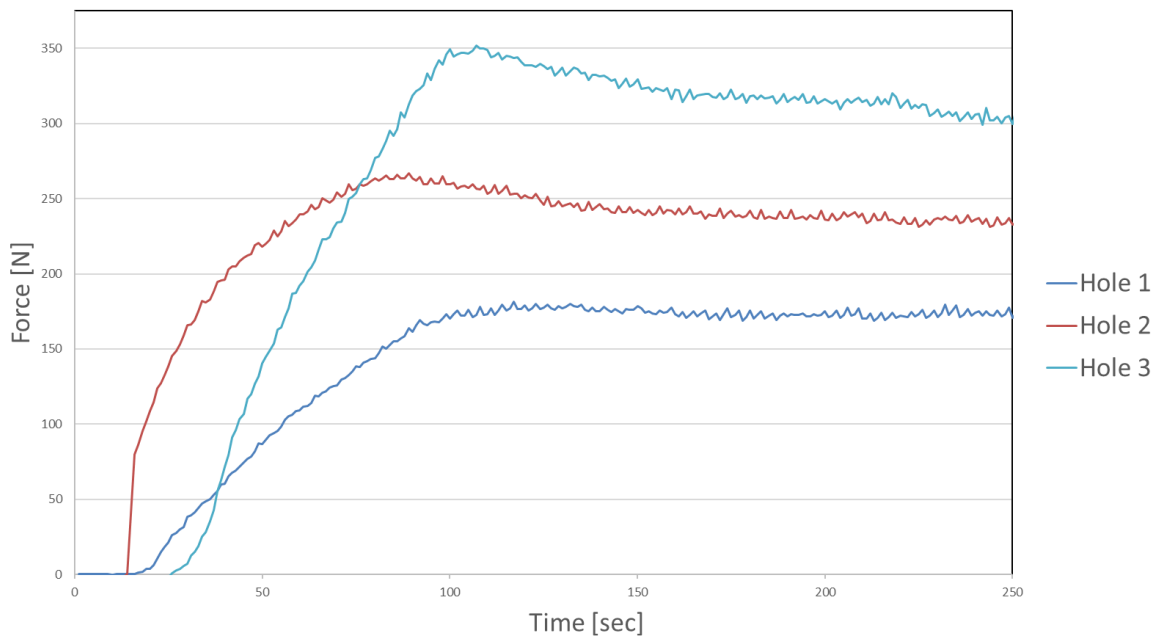


Figure 9. Tool wear present on straight flute bit



The graph in Figure 9 depicts the axial force values of the straight flute drill bit taken every third drill. A significant jump in thrust force occurs due to edge wear; there is substantial degradation to the cutting edge of the bit and significant chipping is present. The distal edges of the flute also show thermal cracking. This damage is likely due to the stiffness of the straight flute bit; due to this stiffness, vibration from the chuck on the hand drill is translated to the cutting edge, causing significant chatter within the drilled hole. This leads to interrupted cutting on the leading edge and excessive heat generation due to friction on the walls of the flank of the drill bit.

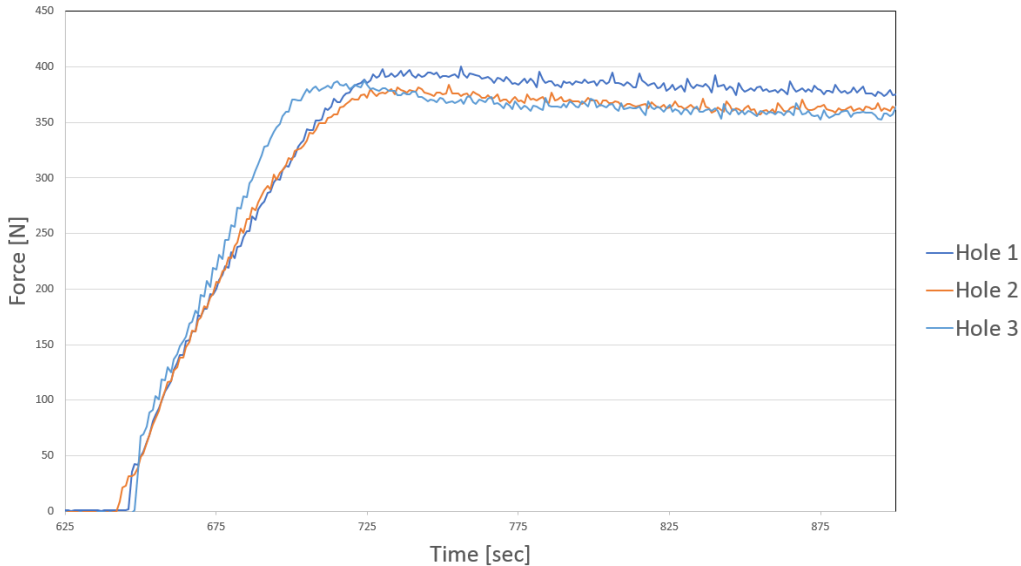


Figure 10. Tool wear present on two-flute twist bit

The graph in Figure 10 shows a direct comparison to the tool wear of the straight flute drill bit. The values graphed were taken every third drill. As depicted, there

is very little tool wear present. This is most likely due to the proper chip evacuation prevent material build up along the cutting edge. The twist drill bit is also markedly more flexible than the straight flute drill bit, meaning less vibrations from the chuck are transmitted to the cutting edge, reducing chatter on the hole wall and reducing interrupted cutting impacts on the surface cutting edge.

#### 4.5 Discussion

All drill bits used in these experiments experienced a significant amount of tool wear relative to their use in an industrial setting. The straight flute drill bit experienced the most wear, nearly doubling the force required to drill within nine drills. The two-flute, though there was some edge degradation over time, was quite consistent with little force increase due to tool wear in the same time frame as the straight flute.

## 5. THERMAL STUDY

### 5.1 Thermal Generation and Propagation

Since a direct measurement at the laser spot during drilling is technically challenging, a calibration curve allows monitoring from a distal measurement. Two thermocouples were used in this calibration test. The localized heat was taken with a thermocouple placed near the center of the sample (denoted as TC1). The second thermocouple (denoted as TC2) was placed at the distal edge of the sample, approximately 11.2 mm away from the first thermocouple. Two tests were repeated: TC1 was placed at 3 mm for the second test while TC2 remained at the same location. The temperature profiles as a function of time are shown in Figure 10. From TC2, it sees a repeatable heating history. The center spot almost immediately heats up to around 500°C after 10 seconds and slowly increases to a maximum of 800°C, while TC2 increases gradually to about 200°C. The second TC1 (at 3 mm from the center) shows a drastic difference from the first TC1 (at center), indicating that the low thermal conductivity of titanium contains the heat at the laser spot and slows down the heat dissipation. This characteristic can minimize the potential thermal damage to the surrounding living tissues in clinical use. However, in this study, to ensure a sufficient temperature rise at the drilling spot, the experiments adopt a long heating with 80 second exposure (expected to be around 800 °C).

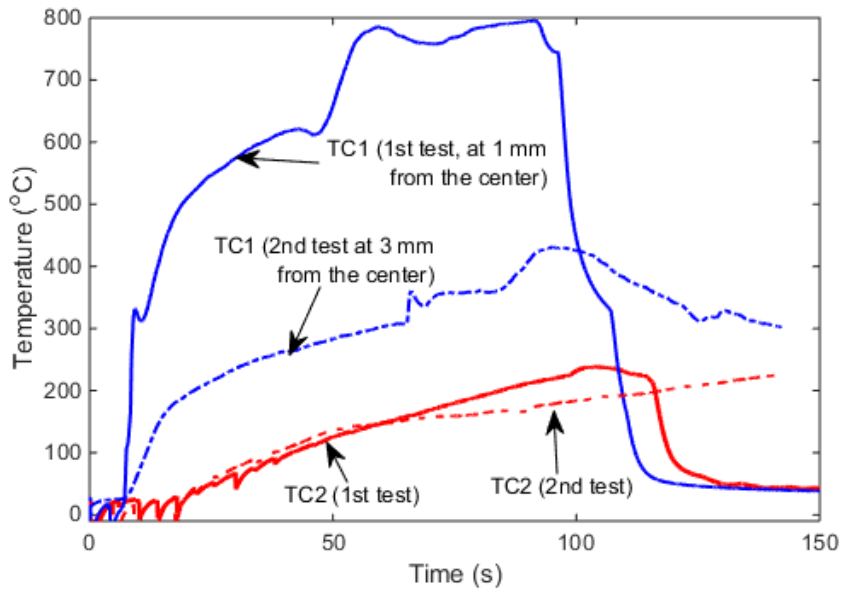
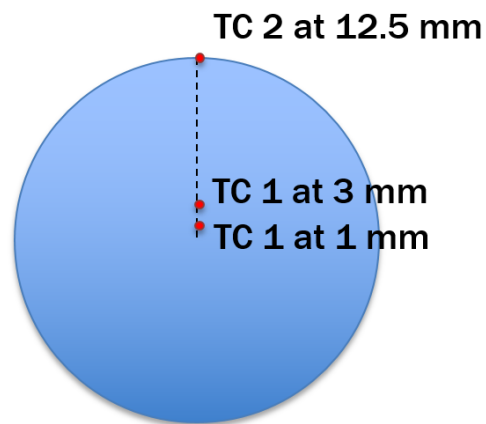


Figure 11. Temperature calibration results of two tests. TC 1 is placed at 1 mm from the laser spot for the first test, 3 mm for the second test. TC2 is replaced at the same distal edge for both tests.



Top down view of workpiece with thermocouple locations

Figure 12. Top down view of thermocouple locations

## 5.2 Abaqus Model

To better understand the gradients present inside the workpiece, numbers that would be difficult to measure experimentally, a Finite Element Analysis (FEA) model was created and analyzed in Abaqus. An axisymmetric model of the workpiece was constructed and given the same material properties as Ti4Al6V. The model was meshed to allow for removal of a discrete amount of the material to replicate chip evacuation while drilling. The boundary condition was set at free convection of titanium into room temperature air.

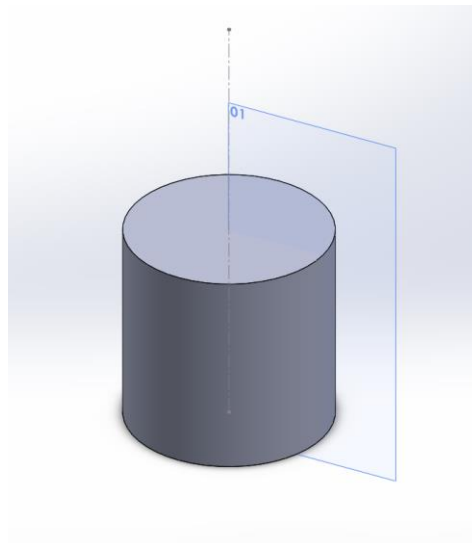


*Figure 13. Model of titanium workpiece*

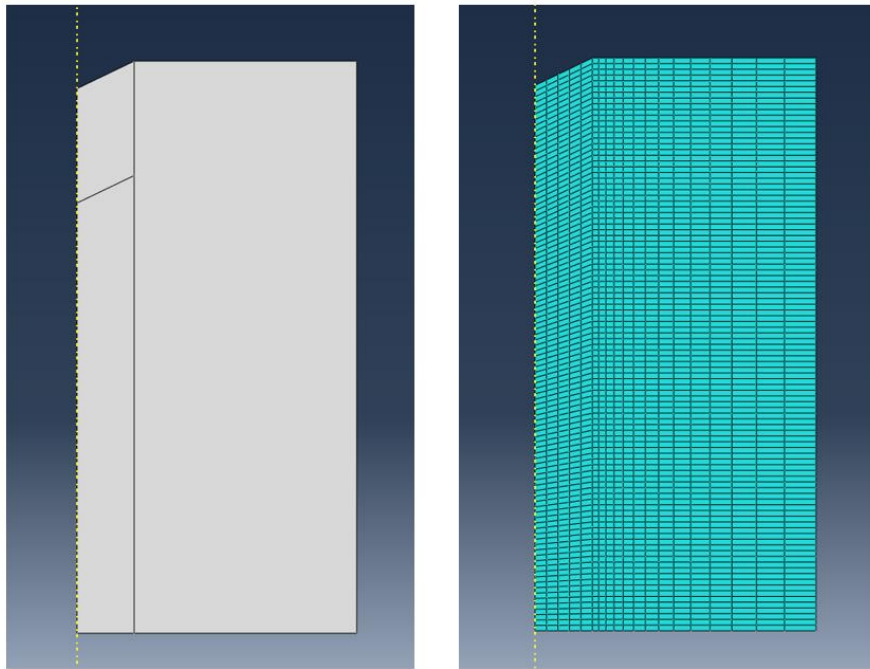


*Figure 14. Axisymmetric model & meshed model*

To replicate the energy input of the laser, a heat flux was applied to the surface of the model, the same size as the laser spot (Figure 14.)

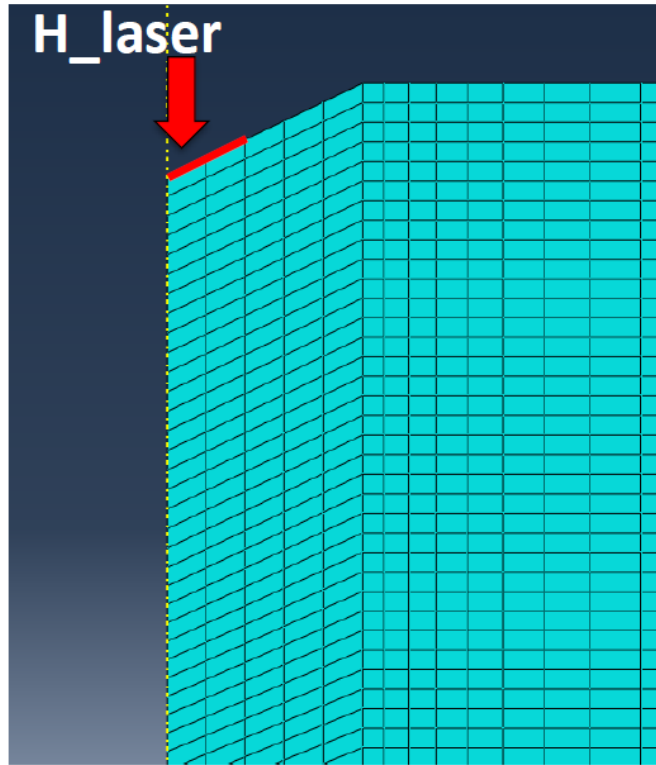


Figure 15. Location of heat flux on the model representing the laser

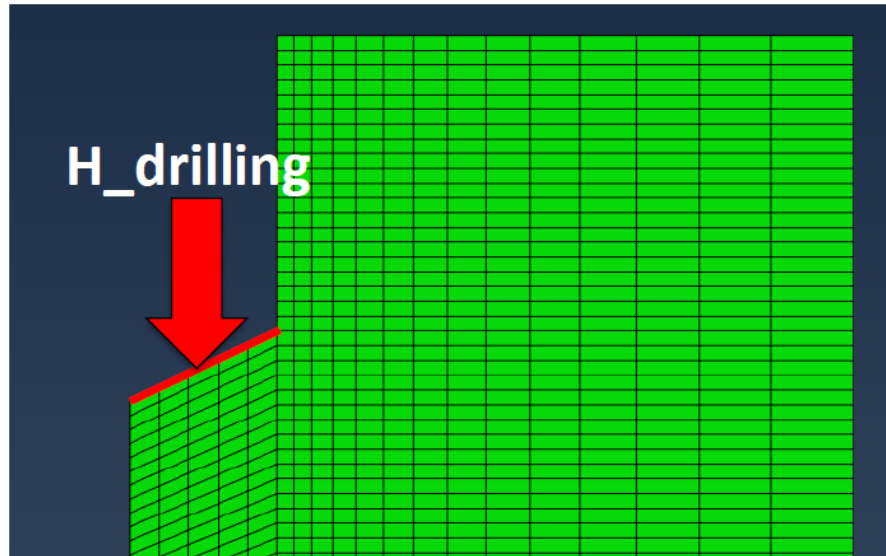


Figure 16. Location of heat flux representative of drilling

To replicate the drilling process, a heat load was created on the surface a diameter of the drill bit (Figure 15.) his load was then applied for a set interval representing the feed rate and time to drill the equivalent distance. The 'chip' was then removed and the process repeated to represent downward drilling progress. Modelling this way allows us to better understand how heat is being generated both via the laser and friction from drilling. We are also able to look at the interior temperatures, values that would be extremely difficult to gather experimental data on.

### 5.3 Inverse Plotting

To validate the results from this model the theoretical outputs from the same thermocouple locations were overlaid as the experimental locations. As depicted, the distal edge value tracks fairly well, as does the 3 mm thermocouple location.



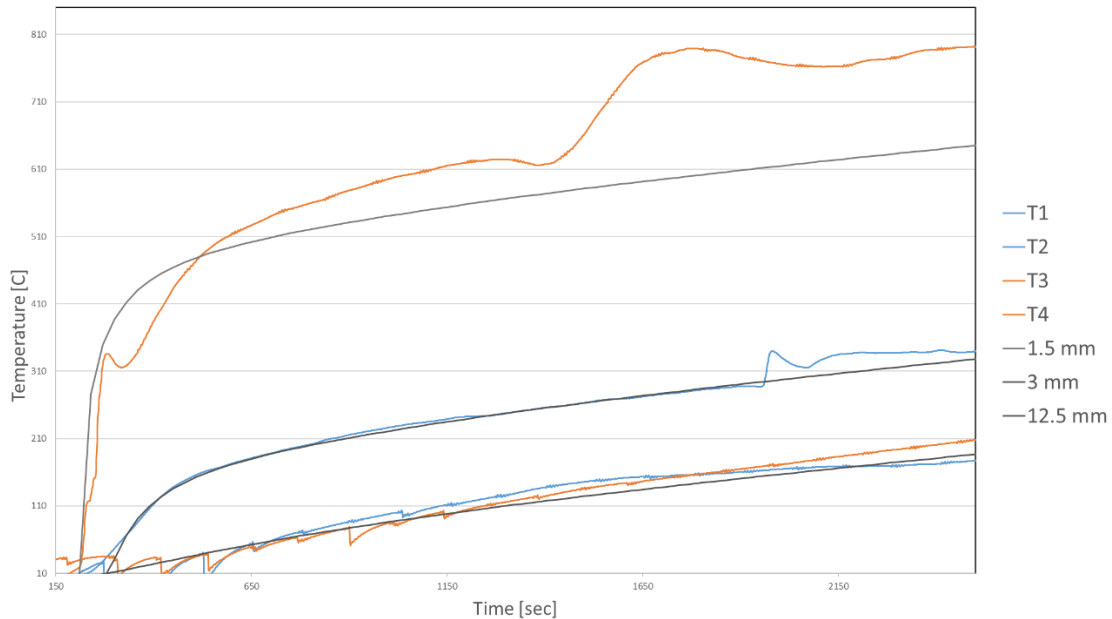


Figure 17. Overlay of experimental temperature data with theoretical data outputted from the model for the laser

The thermocouple located at 1 mm does not track as well, though the overall trend is similar. This can be attributed to the molten pool of the workpiece touching the thermocouple, which explains the sudden spike in temperature. Further tests need to be performed at this location to develop a better understanding of the exact heating profile.

Using the Abaqus model, it was determined that the workpiece was seeing approximately 18.3 watts of energy input. This is roughly 10% of the 200 w power output from the laser. This can be attributed to lack of absorption by the workpiece, possibly due to a highly reflective surface finish or the particular wavelength of the laser. Also, since it is a metal, its reflective value is high, so some of the energy is reflected off instead of being put into the workpiece. This process was repeated

for the temperature rise from just drilling. The thermocouples were placed on the distal edge of the workpiece. The theoretical output of the Abaqus model was overlaid on the experimental data. As depicted, the values correlate well.

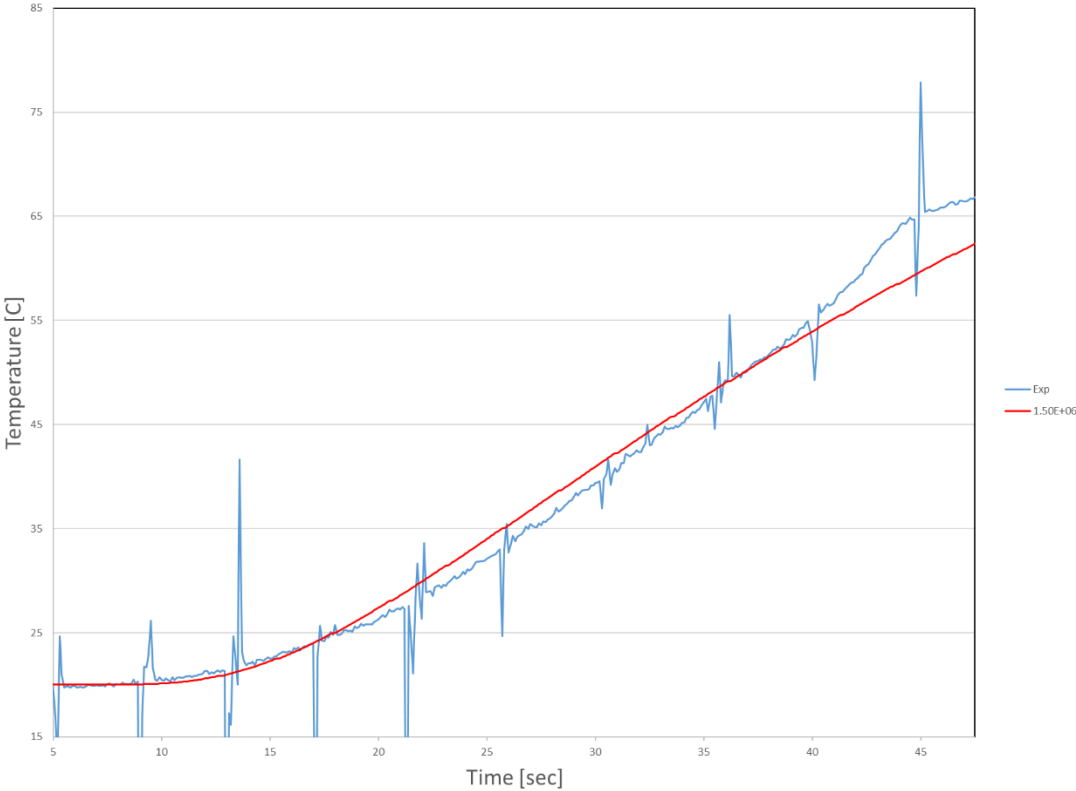
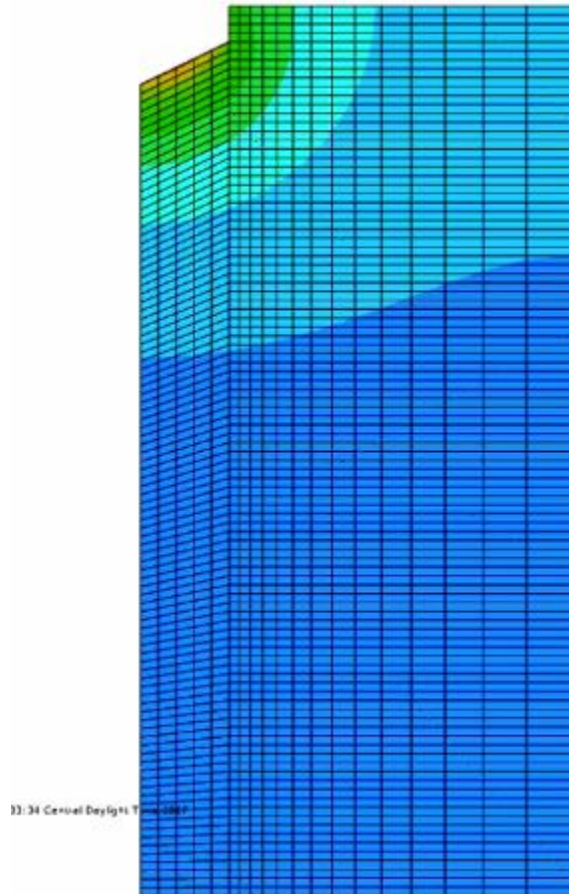


Figure 18. Overlay of experimental data and theoretical model output for drilling

The heat input for drilling is actually larger than the input from the laser. This is a factor that needs to be taken into consideration when looking at drilling from the surgical perspective, as quite a large amount of heat is being generated from just this process alone.

When observing the gradients present inside the material, shown in Figure 18. Below, it is seen that the interior of the workpiece has been raised to a significantly high temperature and then propagates outward.



*Figure 19. Thermal propagation while drilling*

With the distal edge temperature reaching nearly 100°C, thermal management needs to be taken into consideration. As the temperature of the workpiece is above the level at which tissue necrosis occurs, it severely limits the possibility of drilling into titanium implants during surgery.

## 6. DISCUSSION

### 6.1 Discussion

Based on the results, there was an overall thrust force reduction of approximately 10% in the feed direction. Though this is not an insignificant reduction, the total thrust force (over 300 N) is still high and potentially over the limit that a human can produce drilling into the implant without a rigid fixturing mechanism. However, as the drilling was accomplished down to 5 millimeters, it is likely that the full drill engagement has passed the heat zone, meaning the drilling is taking place in a relatively cold titanium sample. By coaxially locating the laser and drill bit, the 2-flute drill bit can potentially decrease to a level of 250 N, which is more likely to be achieved.

From the user perspective, thrust force is a primary indicator, as it shows the amount of force needed to push the drill through, while torque is the major factor from the machining perspective, as it indicates the amount of power needed to drive the tool and cut the material. By looking at the torque data, overall there is a relatively small reduction, likely due to the same issue with the axial direction heat transfer. The torque is calculated after the bit has entered a cooler portion of the sample. Nevertheless, the torque level in general is over 40 Nm, which is considered high for common battery-powered hand drills (10-30 Nm). The exception to this is the torque measurement of the straight flute; the significantly higher torque reading may be explained by the 'gummy' nature of titanium at elevated temperatures. As the straight flute bit has a very low rake angle, it is

possible that the cutting edge was fouled in the initial penetration and continued this process as further drilling took place.

If this project is to be applied in the context clinical processes, a better understanding of the thermal generation needs to be developed. This study demonstrates that the drilling process adds more energy input than does the laser.

It is also important to note that this is the first attempt to explore laser-assisted drilling of prosthetic implants, so this research has several limitations. For example, the sample size may not provide sufficient statistical power to clearly quantify the differences. Furthermore, the potential tool wear is not taken into full account. Also, the limit of a manually-exerted thrust force is unclear, especially under a non-rigid fixturing condition in the human body. Future work will incorporate these factors into the experiment design to further justify these results.

## 7. CONCLUSIONS AND FUTURE WORKS

### 7.1 Conclusions

From the data presented, there is a demonstrable force reduction created by the application of a low powered laser. It can be concluded that with further study, it is possible to drill titanium implants utilizing laser-assisted machining practices; however, drill selection is also critical to maximize its effects. Negative impacts of the straight flute bit were seen in the current study. From a tool design standpoint, an ideal tool would be a coaxial laser-drill system that enables simultaneous heating and drilling, rather than surface heating alone.

Future research will address whether these force and torque values are within the abilities of an average surgeon to reproduce in the operating room by evaluating clinically relevant factors, such as fixturing, force limits, and temperature limits, will must be taken into account.

The two-flute drill, with a considerably better design, is a better choice for drilling multiple holes due to its lack of tool wear. If this is taken out of account, another look should be given to the straight flute design due to its extremely low force values when the bit is new, though this advantage quickly diminishes with each successive hole drilled.

The low absorption rate of the laser causes extended time heating, leading to heat propagation through the workpiece. A critical aspect of the continuation of this study is to increase the adsorption rate of the laser into the workpiece. Our

thermal tests indicate that there is quick increase in localized temperature at the center, and this should be further explored.

## REFERENCES

- [1] Javad P, Vegari D. Periprosthetic Proximal Femur Fractures: Current Concepts. *Journal of Orthopaedic Trauma* 2011;25:
- [2] Pike J, Davidson D, Garbuz D, Duncan CP, O'Brien PJ, Masri BA, Garbuz D. Principles of treatment for periprosthetic femoral shaft fractures around well-fixed total hip arthroplasty. *J Am Acad Orthop Surg* 2009;117:677–88.
- [3] Duncan CP, Masri BA. Fractures of the femur after hip replacement. *Instructor Course Lecture* 1995;44:293–304.
- [4] Corten K, Vanvykel F, Bellemans J, Frederix PR, Simon JP, Broos PL. An algorithm for the surgical treatment of periprosthetic fractures of the femur around a well-fixed component. *Journal of Bone & Joint Surgery* 2009;91:1423–30.
- [5] Bryant GK, Morshed S, Agel J, Henley MB, Barei DP, Taitsman LA, Nork SE. Isolated locked compression plating for Vancouver B1 periprosthetic fractures. *Injury Int J Care Injured* 2009;40:1180–86.
- [6] Walcher M, Giesinger K, du Sart R, Day R, Kuster M. Plate positioning in periprosthetic or interprosthetic femur fractures with stable implants—A biomechanical Study. *The Journal of Arthroplasty* 2016;31:2894-9



- [7] Singh JA, Vessely MB, Harmsen WS, Schleck CD, Melton LJ 3rd, Kurland RL, Berry DJ. A population-based study of trends in the use of total hip and total knee arthroplasty, 1969-2008. *Mayo Clin Proc.* 2010;85:898-904.
- [8] Bashinskaya B, Zimmerman R, Walcott B, Antoci V. Arthroplasty Utilization in the United States is Predicted by Age-Specific Population Groups. *ISRN Orthopedics Volume 2012*;
- [9] Kurtz S, Ong K, Lau E, Mowat F, Halpern M. Projections of primary and revision hip and knee arthroplasty in the United States from 2005 to 2030. *J Bone Joint Surg Am.* 2007;89:780-5.
- [10] Kurtz SM, Lau E, Ong K, Zhao K, Kelly M, Bozic KJ. Future young patient demand for primary and revision joint replacement: national projections from 2010 to 2030. *Clin Orthop Relat Res* 2009;467:2606-12
- [11] Sim, Min S, Choon ML. Determination of optimal laser power according to the tool path inclination angle of a titanium alloy workpiece in laser-assisted machining. *The International Journal of Advanced Manufacturing Technology* 2016;1717-24.
- [12] Sun S, Brandt M, Dargusch MS. Machining Ti-6Al-4V alloy with cryogenic compressed air cooling. *International Journal of Machine Tools and Manufacture* 2010;933-42.

- [13] Bermingham MJ, Kirsch J, Sun S, Palanisamy S, Dargusch MS, New observations on tool life, cutting forces and chip morphology in cryogenic machining Ti-6Al-4V. *International Journal of Machine Tools and Manufacture* 2011;500-11.
- [14] Bermingham MK, Palanisamy S, Kent D, Dargusch MS, A comparison of cryogenic and high pressure emulsion cooling technologies on tool life and chip morphology in Ti-6Al-4V cutting. *Journal of Materials Processing Technology* 2012;752-65.
- [15] Rashid RAR, Sun S, Wang G, Dargusch MS. Machinability of a near beta titanium alloy. *Proceedings of the Institution of Mechanical Engineers, Part B: Journal of Engineering Manufacture* 2011;2151-62.
- [16] Palanisamy S, McDonald SD, Dargusch MS. Effects of coolant pressure on chip formation while turning Ti6-Al-4V alloy. *International Journal of Machine Tools and Manufacture* 2009;739-43.
- [17] Sharif, Safian, and Erween Abd Rahim. Performance of coated-and uncoated-carbide tools when drilling titanium alloy—Ti-6Al4V. *Journal of Materials Processing Technology* 2007;72-6.
- [18] Baskar, N. Comparison of coated and uncoated carbide drill bits for drilling titanium grade 2 material. *Mechanics* 2016;571-5.

- [19] Sushinder K, Shicaram PR, Nivedh Kannaa SB, Investigation of Thrust forces, Torque and Chip microstructure during Drilling of Ti-6Al-4V Titanium alloy. *Applied Mechanics & Materials* 2015;
- [20] Waqar S, Asad S, Ahmad S, Abbas A, Elahi H. Effect of Drilling Parameters on Hole Quality of Ti-6Al-4V Titanium Alloy in Dry Drilling. *Materials Science Forum*. 2017;
- [20] Chang C-W, Kuo C-P. Evaluation of surface roughness in laser-assisted machining of aluminum oxide ceramics with taguchi method. *Int. J. Mach. Tools Manuf.* 2007;47:141–7.
- [21] Ding H, Shen N, Shin YC. Thermal and mechanical modeling analysis of laser- assisted micro-milling of difficult-to-machine alloys. *J. Mater. Process. Technol.* 2012;601–13
- [22] Rahman RAR, Sun S, Wang G, Dargusch MS. An investigation of cutting forces and cutting temperatures during laser-assisted machining of the Ti–6Cr–5Mo–5V–4Al beta titanium alloy. *International Journal of Machine Tools and Manufacture* 2012;63:58-69.
- [23] Ayed Y, Germain G, Salem B, Hamdi. Experimental and numerical study of laser-assisted machining of Ti6Al4V titanium alloy. *Finite Elements in Analysis and Design* 2014;92:72-9.

- [24] Sun S, Brandt M, Barnes JE, Dargusch MS. Experimental investigation of cutting forces and tool wear during laser-assisted milling of Ti-6Al-4V alloy. Proceedings of the Institution of Mechanical Engineers, Part B: Journal of Engineering Manufacture 2011;225:1512-27.
- [25] Suthar K, Patten J, Dong L, Abdel-Aal H. Estimation of temperature distribution in silicon during micro laser assisted machining. Proceedings of the 2008 International Manufacturing science and engineering conference MSEC 2008;
- [26] Yang J, Sun S, Brandt M, Yan W. Experimental Investigation and 3D finite element prediction of heat affected zone during laser assisted machining of Ti6Al4V alloy, Journal of Material Processing Technology 2010;210:2215-22.
- [27] Joshi A, Kansara N, Das S, Kuppan P, Vankatesan K. A Study of Temperature Distribution for Laser Assisted Machining of Ti-6Al-4V Alloy. Procedia Engineering 2014;97:1466-73.
- [28] Rashid RAr, S.Sun, G.Wang, M.S. Dargusch, Effect of laser power on machinability of Ti6Cr5Mo5V4Al beta titanium alloy during laser assisted machining, International Journal of machine tools and manufacture 2012;63:41-3.

- [29] Rashid RAR, Sun S, Palamisamy S, Wang G, Dargusch MS. A study on laser assisted machining of Ti10V2Fe3Al alloy with varying laser power. *The International Journal of Advanced Manufacturing Technology* 2014;219-24.
- [30] Zamani H, Hermani JP, Sonderegger B, Sommitsch C. 3D simulation and process optimization of laser assisted milling of Ti6Al4V. *Proced. CIRP* 2013;8:75–80.